

Calibration and Verification of a Hydrodynamic Model  
in Chunsu Bay and Adjacent Coastal Water  
천수만과 인근연안에서 수역학모델의 보정 및 검증

Kyeong Park\* and Jeong-Hwan Oh\*\*

박 경\* · 오정환\*\*

**Abstract** □ A horizontal two-dimensional version of POM (Princeton Ocean Model) was modified in representing the bottom friction and the open boundary conditions. To simulate the flooding and drying of intertidal flats, a wetting-and-drying scheme was incorporated into the model. The model then was applied to the Chunsu Bay and its adjacent coastal water. Only the water movement due to tides, the dominant forcing in the study area, was considered. This paper presents the procedure and the results of model calibration and verification for the Chunsu Bay system. The model was calibrated, using the average tidal characteristics in Tide Tables, for the amplitudes and the phases of tidal waves throughout the modeling domain. Calibration results showed that the model gave a good reproduction of tidal waves. The calibrated model was verified using the time-series measurements of surface elevation and current velocity in the summer of 1995. The model reproduced the tides and tidal currents very well. Calibration and verification results demonstrated that the model is capable of reproducing the tidal dynamics in the Chunsu Bay system.

**Keywords** : numerical model, model calibration, model verification, field data, wetting-and-drying scheme

**요** **요** : 수평 2차원 POM(Princeton Ocean Model)을 바닥마찰과 개방경계조건에 대하여 수정하고, 간석지를 모의하기 위하여 wetting-and-drying 기법을 첨가하여 천수만과 인근연안에 적용하였다. 연구해역의 주된 기작인 조석에 의한 해수유동만을 고려하였다. 본 논문은 천수만 해역에서의 모델 보정과 검증 절차 및 결과를 제시한다. 조석표의 평균 조석 특성을 이용하여 모델영역 전반에 걸쳐 진폭과 위상을 포함하는 조석파의 전파에 대하여 모델을 보정하였고, 보정 결과가 조석파를 잘 재현하였다. 보정된 모델을 1995년 여름 관측된 해수면 변위와 유속에 대한 시계열 자료를 이용하여 검증하였고, 검증 결과가 조석 및 조류를 잘 재현하였다. 보정 및 검증 결과가 본 모델이 천수만 해역에서 조석 현상을 잘 재현할 수 있음을 보여주었다.

**핵심용어** : 수치모델, 모델 보정, 모델 검증, 관측자료, 간석지 처리 기법

## 1. INTRODUCTION

Transport and distribution of dissolved and particulate materials in coastal waters, which draw more and more attention in recent years, are greatly influenced by water movement (Park, 1996). Water movement in coastal

waters is affected by various forcings such as tides, freshwater inflows, waves, winds and land boundaries, and thus are always in transitional state, never reaching steady state. Numerical hydrodynamic models have been widely used to study the water movement and the associated transport of materials in coastal waters (e.g.,

\*인하대학교 해양학과 (Department of Oceanography, Inha University, 253 Yonghyun-dong, Nam-gu, Incheon 402-751, Korea)

\*\* (주)삼우환경컨설팅 (Samwoo Environmental Consultant Corporation, POSPO B/D 401, 1364-42 Seocho-dong, Seocho-gu, Seoul 137-070, Korea)

Oey *et al.*, 1985; Galperin and Mellor, 1990; Park *et al.*, 1991; Jung and Yoa, 1992; Cheng *et al.*, 1993; Kim, 1994; Kim *et al.*, 1994; Lee, 1994; Park and Kuo, 1994; Park *et al.*, 1996).

Since our current understanding of prototype processes is far from complete, neither are numerical models that directly reflect our incomplete understanding. Numerical hydrodynamic models hence inherently contain some coefficients (e.g., bottom friction coefficient, vertical mixing coefficient, etc.), of which we have limited understanding and know only the ranges of their magnitudes. We also can never have a complete set of field data to specify initial conditions throughout the modeling domain (especially for masses such as salinity and temperature) and boundary conditions throughout the model run, which makes us to estimate initial and boundary conditions based on available field data. Therefore, a numerical model, whenever applied to a system, should be calibrated and verified with field data, so as to reliably evaluate the uncertain coefficients and to examine the reliability of the estimated initial and boundary conditions, with the aid of field data.

Many studies using numerical models have been conducted for Korean coastal waters to try to understand prototype processes, but not all have tried to calibrate and verify the applied models. Such modeling applications that have not been supported by calibration and verification have not been able to provide measures of the degree of reliability of model results, degrading the reliability of any outputs derived from the model results. Ideally speaking, whenever a numerical model is applied to a coastal system, a comprehensive field survey should be implemented to collect field data specifically for the purpose of model calibration and verification, which has not been possible in most model applications for Korean coastal waters. Nonetheless, we believe that the quantity and quality of currently available data for tides and currents in most Korean coastal waters do allow us to perform model calibration and verification to some degree. We cannot expect that this type of model calibration and verification with field data that have not been collected

specifically for modeling purposes gives flawless results. However, calibration and verification of numerical models should be carried out with whatever field data that might be available, and the results should be presented to provide measures of the degree of reliability of model results.

Model calibration is the process, in which we evaluate the uncertain coefficients and to examine the reliability of the estimated initial and boundary conditions by comparing the model results with the field data. Hence, it would be desirable to calibrate a model such that the model's capability of reproducing the mean observed conditions throughout the modeling domain can be examined. For coastal waters, the Tide Tables provide the average tidal characteristics (i.e., amplitudes and phases of important tidal harmonic constituents) from stations along the coast. Such data, when used for model calibration, enable us to examine both the amplitudes and the phases of tidal waves in the modeling domain. Thus, model calibration using average tidal characteristics would be ideal for coastal waters. The model calibration alone does not guarantee that the validity of the model can be extended beyond the data set used in the calibration process. Hence, the validity of model calibration, that is the adequacy and consistency of the calibrated coefficients, should be verified using an independent set of field data. Verification is the process, in which we compare the model results generated without changing the coefficient values determined in calibration with the verification data set. An independent data set, again from the entire modeling domain, would be perfect for verification, which in most cases is not available. Then, time-series data of surface elevation and current velocity from several locations in the modeling domain may be used for model verification.

A horizontal two-dimensional version of POM (Princeton Ocean Model) was modified in representing the bottom friction and the open boundary conditions, and to incorporate wetting-and-drying scheme for intertidal flats. The model was applied to the Chunsu Bay and its adjacent coastal water (hereafter referred to

as the Chunsu Bay system). Only the water movement due to tides, the dominant forcing in the study area, was considered, and the effects of wind stress and density gradient were neglected. The model was calibrated using the average tidal characteristics in Tide Tables, and the calibrated model was verified using the time-series measurements of surface elevation from three stations and current velocity from five stations in the summer of 1995. This paper presents the procedure and the results of model calibration and verification for the Chunsu Bay system.

## 2. STUDY AREA

The Chunsu Bay, located at the central part of the west coast of Korea Peninsula, is a semi-enclosed

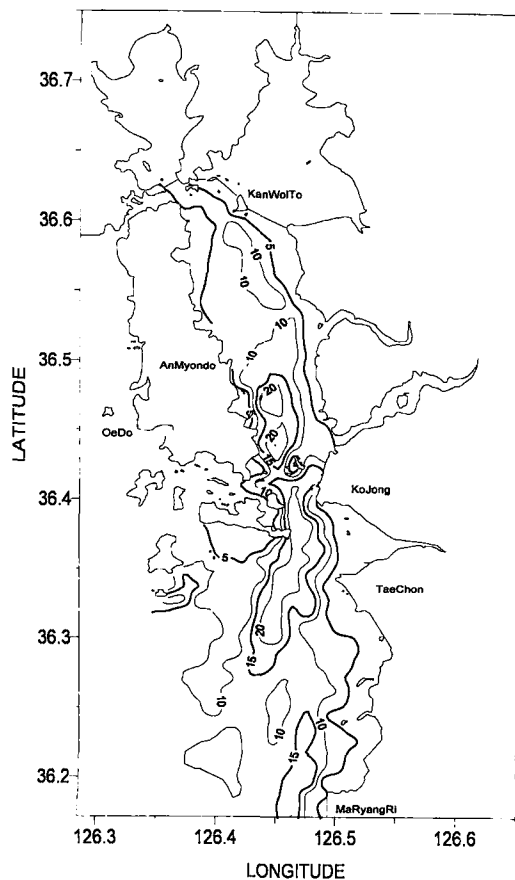


Fig. 1. Chunsu Bay system: contours are water depth (m) relative to lower low water.

coastal body (Fig. 1). The length of the Chunsu Bay in the north-south direction is about 40 km from the Bay mouth near Kojong, and the maximum width in the east-west direction is about 10 km. A distinct tidal channel is developed from adjacent coastal water into the Bay, which facilitates the flushing of Bay water. The average depth relative to mean sea level is about 10 m with the deepest part of 30 m at the Bay mouth. The Chunsu Bay system has complex shoreline configuration with islands, sand ridges and reefs. The Chunsu Bay system has been known as a good spawning ground and to contain a variety of valuable living resources. Two embayments at the head of the Bay were disconnected from the Bay by constructing dams and making two freshwater lakes in 1985, which have changed the circulation pattern and the bottom topography in the Chunsu Bay system. Discharge of excess water from two lakes through floodgates during wet season has been believed to degrade the water quality in the Chunsu Bay system.

There are three reference tide gauge stations at the Chunsu Bay system: Taechon (just outside of the Bay), Kojong (Bay mouth) and Kanwolto (head of the Bay). Tidal system at the Chunsu Bay system is dominated by semidiurnal tides with the amplitudes of 2.3 and 0.9 m, respectively, for  $M_2$  and  $S_2$  tides at Kojong, while  $K_1$  and  $O_1$  tides respectively have the amplitudes of 0.4 and 0.3 m (KORDI, 1996). Tidal ranges are 6.4 m during spring tide and 2.8 m during neap tide. Because of the large tidal range, extensive intertidal flats are developed along the shoreline. Maximum flooding and ebbing currents inside the Bay are 1.2 knots and 1.9 knots respectively, and narrow tidal channel strengthens currents at the Bay mouth with the maximum flooding and ebbing currents of 3.6 knots and 3.1 knots respectively (Office of Hydrographic Affairs, 1992).

Long-term average surface temperature is  $16.6^\circ\text{C}$  with the minimum of  $5.0^\circ\text{C}$  in March and the maximum of  $27.0^\circ\text{C}$  in August (KORDI, 1997). Temporal variations in salinity are relatively small, probably owing to the reduction in freshwater discharge resulted from the construction of two dams at the head of the Bay, ranging

from 31.3 psu in August and 32.5 psu in October (Yoo, 1992). Both horizontal and vertical gradients are less than 1°C for temperature and 0.5 psu for salinity. Small horizontal gradient in salinity is again due to the construction of two dams at the head of the Bay. Small vertical gradients for both temperature and salinity are due to the strong vertical mixing resulted from strong tidal current.

### 3. MODEL DESCRIPTION

A horizontal two-dimensional version of POM was modified in representing the bottom friction and the open boundary conditions, and to incorporate wetting-and-drying scheme for intertidal flats. A brief description of the model, mainly for the modifications made, is given below. The governing equations consisting of continuity and momentum equations are:

$$\frac{\partial \eta}{\partial t} + \frac{\partial DU}{\partial x} + \frac{\partial DV}{\partial y} = 0 \quad (1)$$

$$\begin{aligned} \frac{\partial U D}{\partial t} + \frac{\partial U U D}{\partial x} + \frac{\partial U V D}{\partial y} - f V D = -g D \frac{\partial \eta}{\partial x} + \frac{1}{\rho_o} \tau_x^w \\ - \frac{1}{\rho_o} \tau_x^b + \frac{\partial}{\partial x} \left( 2 D A_M \frac{\partial U}{\partial x} \right) + \frac{\partial}{\partial y} \left( D A_M \left[ \frac{\partial U}{\partial y} + \frac{\partial V}{\partial x} \right] \right) \end{aligned} \quad (2)$$

$$\begin{aligned} \frac{\partial V D}{\partial t} + \frac{\partial U V D}{\partial x} + \frac{\partial V V D}{\partial y} + f U D = -g D \frac{\partial \eta}{\partial y} + \frac{1}{\rho_o} \tau_y^w \\ - \frac{1}{\rho_o} \tau_y^b + \frac{\partial}{\partial y} \left( 2 D A_M \frac{\partial V}{\partial y} \right) + \frac{\partial}{\partial x} \left( D A_M \left[ \frac{\partial U}{\partial y} + \frac{\partial V}{\partial x} \right] \right) \end{aligned} \quad (3)$$

where  $t$ =time;  $x$ =east-west coordinate;  $y$ =north-south coordinate;  $\eta$ =surface elevation;  $D$ =total depth;  $U$  and  $V$ =vertically averaged horizontal velocities in  $x$  and  $y$  directions, respectively;  $f$ =Coriolis parameter;  $g$ =gravitational constant;  $\rho_o$ =mean density;  $\tau_x^w$  and  $\tau_y^w$ =wind stress in  $x$  and  $y$  directions, respectively;  $\tau_x^b$  and  $\tau_y^b$ =bottom frictional stress in  $x$  and  $y$  directions, respectively;  $A_M$ =horizontal eddy viscosity. POM estimates the horizontal eddy viscosity ( $A_M$ ) using the scales of motion being resolved in the model and the local deformation field as suggested by Smagorinsky

(1963):

$$A_M = C \cdot \Delta x \Delta y \left[ \left( \frac{\partial U}{\partial x} \right)^2 + \frac{1}{2} \left( \frac{\partial U}{\partial y} + \frac{\partial V}{\partial x} \right)^2 + \left( \frac{\partial V}{\partial y} \right)^2 \right]^{1/2} \quad (4)$$

where  $\Delta x$  and  $\Delta y$ =grid intervals in  $x$  (east-west) and  $y$  (north-south) directions, respectively;  $C$ =Smagorinsky constant (ca. 0.2).

Two-dimensional version of POM expresses the bottom frictional stress using the quadratic stress law with the friction coefficient quantified using the constant drag coefficient. We modified POM such that the friction coefficient is expressed using the Manning's friction coefficient (Daily and Harleman, 1966), which accounts for the effects of variations in depth on bottom frictional stress. At the open boundary, POM uses the nonlinear advective part of momentum equation to evaluate the tangential velocity and the radiation condition for normal velocity. We modified POM such that momentum equations without the horizontal advective and diffusive terms are solved to evaluate the normal open boundary velocity.

POM uses staggered Arakawa C-grid, and Fig. 2 shows the grid system with the location of variables. Governing equations are cast into their flux-conservative forms, and integrated over a cell volume. POM solves the surface slope term (barotropic forcing term) in momentum equations semi-implicitly, by

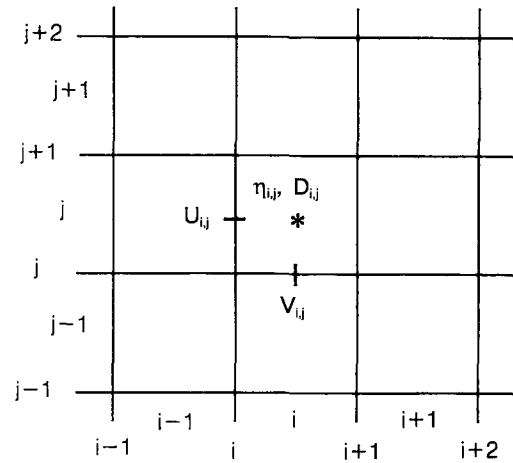


Fig. 2. Arakawa C-grid system showing the positions of the variables.

employing the weighted mean values of the surface elevations from three time-levels (i.e., old, present and new time steps). Horizontal advection and diffusion terms are solved using central difference scheme, and the time derivative terms are solved using three time-level leapfrog scheme, both of which have the second-order accuracy. Weak time-filter proposed by Asselin (1972) is used to remove computational mode caused by leapfrog scheme. A more detailed description of original POM can be found in Blumberg and Mellor (1987) and Mellor (1996).

A numerical model that cannot represent shallow intertidal zones appropriately cannot reproduce the propagation of the tidal waves in coastal waters (Kuo and Park, 1995). To account for the extensive intertidal flats along the west coast of Korea Peninsula, the wetting-and-drying scheme proposed by Flather and Heaps (1975) was slightly modified and incorporated into the present model. In determining wet or dry status at the locations where velocities are defined (Fig. 2), if the condition in Eq. (5) is not satisfied, the  $i^{\text{th}}$  location is considered to be dry and velocity is set to zero.

$$D_{i-1}^{n+1} > D_C \text{ and } D_i^{n+1} > D_C \quad \text{or}$$

$$D_{i-1}^{n+1} < D_C \text{ and } D_i^{n+1} > D_C \text{ and } \eta_i^{n+1} - \eta_{i-1}^{n+1} > \epsilon \text{ or}$$

$$D_{i-1}^{n+1} > D_C \text{ and } D_i^{n+1} < D_C \text{ and } \eta_i^{n+1} - \eta_{i-1}^{n+1} > \epsilon \quad (5)$$

where  $D_C$ =critical depth;  $\epsilon$ =critical surface gradient; the subscript  $i-1$  and  $i$  are cell indexes; the superscript  $n+1$  denotes the future time step. The model application described below showed that the model results were insensitive to the selection of  $D_C$  and  $\epsilon$ : we used  $D_C=0.1$  m and  $\epsilon=0.1$  m. The behavior of the wetting-and-drying scheme in the present model application is discussed below.

#### 4. MODEL APPLICATION

The coastal region between  $36^{\circ}10'-36^{\circ}33'N$  and  $126^{\circ}22'-126^{\circ}33'E$  was selected as the modeling domain (Fig. 3), partly dictated by the availability of the data for open boundary conditions. The modeling domain was

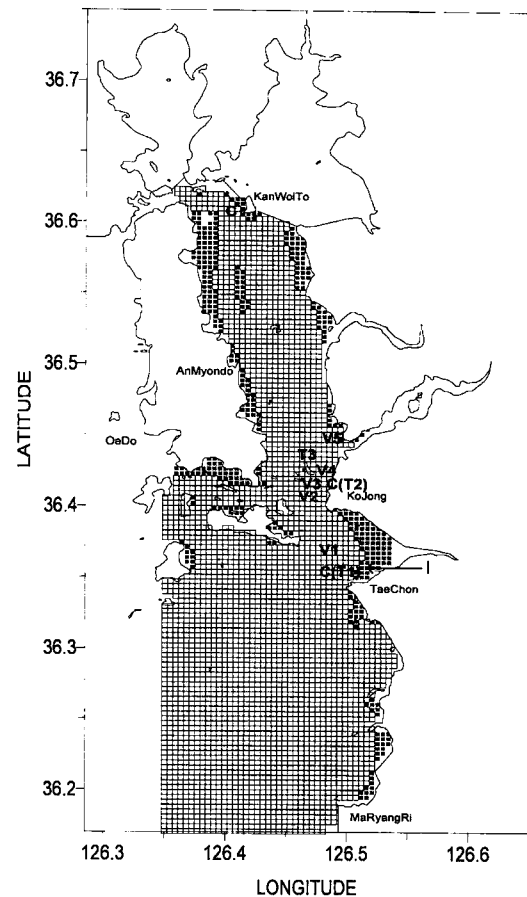


Fig. 3. Grid structure showing the locations of calibration stations (three C's), and verification stations for surface elevation (T1 to T3) and for current velocity (V1 to V5). Dark areas indicate intertidal flats.

gridded with  $\Delta x$  and  $\Delta y$  of 500 m, resulting in  $44 \times 133$  total cells with 3273 active water cells including 404 intertidal cells. Five seconds of time step was used, which satisfied the CFL stability condition. As initial conditions of surface elevation and velocity, arbitrary values were specified for both calibration and verification runs (cold start). Since it took less than 5 days for the model to overcome completely the effect of initial conditions, only the model results after 5 days since the model started were used. For this study, the wind stress was not considered.

The model was forced with the tide generated with harmonic constants of four major tidal constituents ( $M_2$ ,  $S_2$ ,  $K_1$  and  $O_1$ ) along the open boundary cells:

$$\eta(x, y, t) = \sum_i^4 f_i \cdot a_i \cdot \cos(\omega_i t - k_i + E_i + u_i) \quad (6)$$

where  $a_i$ ,  $\omega_i$ ,  $k_i$ ,  $f_i$  and  $E_i + u_i$  are amplitude, angular velocity, phase lag, node factor and astronomical argument of the  $i^{\text{th}}$  tidal constituents, respectively. The node factors, which are small adjustments to the amplitudes to allow for modulations over the 18.6-year nodal period, are taken to be unity in this model application (Pugh, 1987). The astronomical arguments of four major tidal constituents were computed following Dronkers (1964). Data of harmonic constants ( $a_i$  and  $k_i$ ) for four major tidal constituents were obtained from KORDI (1996) at Maryangri, southeast end of boundary, and Oedo, northwest end of boundary (Fig. 3). Since the harmonic constants at these two boundary locations showed very little differences (Table 1), average values of the two were used uniformly along the open boundary cells.

To show the behavior of the implemented wetting-and-drying scheme (Eq. 5), the time-series plots of surface elevation and current velocity at the intertidal cell I (Fig. 3) are presented in Fig. 4. While the intertidal cell is dry, the velocity components become zero, and as the cell gets wet again, the water resumes to flow. When the water depth in an intertidal cell becomes very shallow either in rising or falling tide, small fluctuations in velocity are observed in model behavior. Such fluctuations, caused by surface elevation and velocity components being defined at different locations in C-grid (Fig. 2), sometimes may affect the surface elevation such that they may cause alternations between wet and dry status, as was noted by Leendertse and Gritton (1971). In Fig. 4, however,

**Table 1.** Observed harmonic constants at Maryangri and Oedo: see Fig. 3 for locations

Tidal Constituents	Maryangri		Oedo	
	Amplitude (m)	Phase (deg.)	Amplitude (m)	Phase (deg.)
$M_2$	2.10	80.4	2.10	90.3
$S_2$	0.83	128.9	0.73	135.0
$K_1$	0.35	273.7	0.35	274.0
$O_1$	0.27	236.2	0.27	248.2

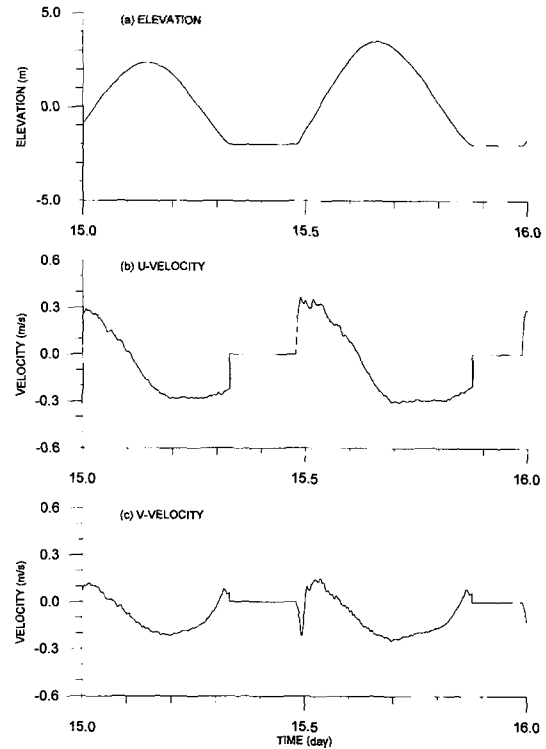


**Fig. 4.** Time series plots of (a) surface elevation, (b) u-velocity and (c) v-velocity at an intertidal cell (location I in Fig. 3).

the small fluctuations in velocity neither persist nor affect the surface elevation. The location of the intertidal cell I (Fig. 3) is carefully chosen so that we can compare the results in Fig. 4 with those at nearby water cells such as C, T1 and V1 (Fig. 3). The small fluctuations at the intertidal cell I do not propagate into the nearby water cells, and hence the present wetting-and-drying scheme gives satisfactory performance at least for the present model application.

#### 4.1 Model Calibration

The present model has two calibration parameters that need to be determined, the Manning's friction coefficient and the Smagorinsky constant (Eq. 4). For the latter, 0.2 is taken following Smagorinsky (1963). Then, the model was calibrated to evaluate the Manning's coefficient using the average tidal information in the Chunsu Bay system. The observed amplitudes and phases of  $M_2$ ,  $S_2$ ,  $K_1$  and  $O_1$  constituents were available

at three reference tide gauge stations: Taechon (outside of the Bay), Kojong (Bay mouth) and Kanwolto (head of the Bay). The locations of these three calibration stations (Fig. 3) are suitable to examine the propagation of the incident and reflected tidal waves throughout the modeling domain. The amplitudes and phases of four major tidal constituents, obtained from harmonic analysis of the model results for 28 days, were compared to the observed ones from three stations. The Manning's coefficient was adjusted, within the range of commonly accepted values (typically 0.01 to 0.04 in coastal waters), until the computed amplitudes and phases agreed with the observed ones. As a result of calibration, the Manning's coefficient was determined to be 0.025.

The model calibration results at three stations are compared with the observations in Fig. 5. As quantitative measures of model calibration, error (E) was computed using Eq. (7) for amplitude and phase, and absolute relative error (ARE) was computed using Eq. (8) for

amplitude. The results are presented in Table 2. ARE is a measure of the absolute difference between observations and model results and ARE of zero is ideal. Positive E indicates the model's overprediction of the observations and negative E indicates the model's underprediction of the observations.

$$E = P_i - O_i \tag{7}$$

$$ARE (\%) = \frac{|O_i - P_i|}{|O_i|} \times 100 \tag{8}$$

where  $O_i$  and  $P_i$ =observation and model result respectively.

The calibration results show a good agreement between model results and field data for both amplitudes and phases at Taechon and Kojong. At Kanwolto, the computed amplitudes are in a good agreement with the data, but the model somewhat underestimates the phases (i.e., tidal waves in the model propagate somewhat faster than those observed). The calibration results in Fig. 5 and Table 2 show that the model gives a good reproduction of tidal waves in the Chunsu Bay system.

#### 4.2 Model Verification

Verification compares the model results generated without changing the Manning's friction coefficient determined in calibration (0.025) with the independently collected verification data set. In this study, the time-series measurements of surface elevation and current velocity in summer of 1995 (KEPCO, 1996) were used for model verification. Surface elevation was measured from three stations (T1 to T3 in Fig. 3) and current velocity was measured from surface and bottom of five stations (V1 to V5 in Fig. 3). The sampling period covered from August 20 to September 18 in 1995. For verification, the model was run from August 15 to September 19 in 1995, so that the model results from August 20, which are free from the effect of arbitrary specified initial conditions, were used for model-field comparison. The model was forced with the open boundary conditions generated with Eq. (6) for four major tidal constituents, in which the astronomical

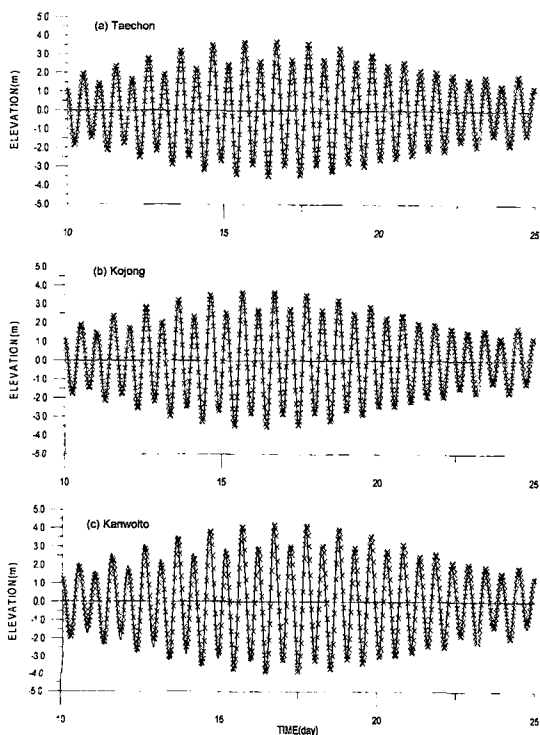


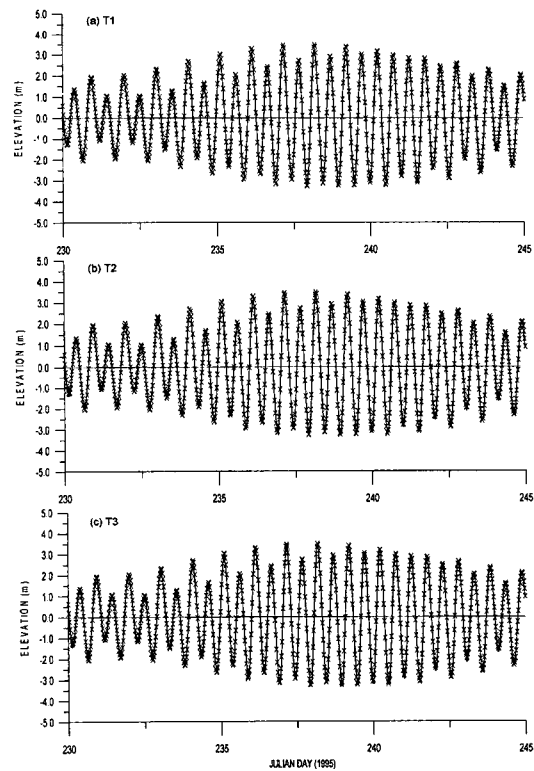
Fig. 5. Calibration results for surface elevations at (a) Taechon, (b) Kojong and (c) Kanwolto. Solid lines are model results and × marks are field data.

**Table 2.** Comparison between observations and model results of amplitudes and phases for four major tidal constituents at three calibration stations

Calibration Stations		Taechon		Kojong		Kanwolto	
		Data	Model	Data	Model	Data	Model
$M_2$	Amplitude (m)	2.37	2.22	2.29	2.30	2.56	2.47
	ARE (%)		6.3		0.4		3.5
	Error (m)		-0.15		0.01		-0.09
	Phase (deg.)	88.6	88.1	87.0	91.1	107.1	94.8
	Error (deg.)		-0.5		4.1		-12.3
$S_2$	Amplitude (m)	0.83	0.83	0.89	0.86	1.01	0.93
	ARE (%)		0.0		3.4		7.9
	Error (m)		0.00		-0.03		-0.08
	Phase (deg.)	140.8	135.7	130.8	139.8	170.0	144.6
	Error (deg.)		-5.1		9.0		-25.4
$K_1$	Amplitude (m)	0.38	0.35	0.36	0.35	0.48	0.36
	ARE (%)		7.9		2.8		25.0
	Error (m)		-0.03		-0.01		-0.12
	Phase (deg.)	271.4	275.5	276.4	277.5	287.7	279.6
	Error (deg.)		4.1		1.1		-8.1
$O_1$	Amplitude (m)	0.27	0.27	0.27	0.27	0.28	0.28
	ARE (%)		0.0		0.0		0.0
	Error (m)		0.00		0.00		0.00
	Phase (deg.)	246.5	244.0	248.4	246.2	254.2	248.2
	Error (deg.)		-2.6		-2.2		-6.0

arguments in Eq. (6) were computed following Dronkers (1964) for the period of verification run.

The model runs in this study include only the tidal forcing by four major tidal constituents ( $M_2$ ,  $S_2$ ,  $K_1$  and  $O_1$ ), and thus the model results reflect only the response of the system to the imposed tidal forcing. In the prototype however other tidal forcings, baroclinic forcing due to horizontal density gradient, freshwater discharges, winds, etc., also affect the water movement. Therefore, harmonic analysis was conducted to find the harmonic constants for four major tidal constituents from the observed time-series data. Then, the field data were reconstructed using the four major tidal constituents and compared with the model results from the verification run. Fig. 6 presents the verification results for surface elevation at stations T1 to T3, respectively. The results indicate that the model gives a good reproduction of tides for both amplitudes and phases. Fig. 7 presents the verification results for current velocity at stations V2, V3 and V5 respectively. The slight model-field discrepancies in Fig. 7 may be explained in terms of the following two points. One is

**Fig. 6.** Verification results for surface elevations at (a) T1, (b) T2 and (c) T3. Solid lines are model results and  $\times$  marks are field data.



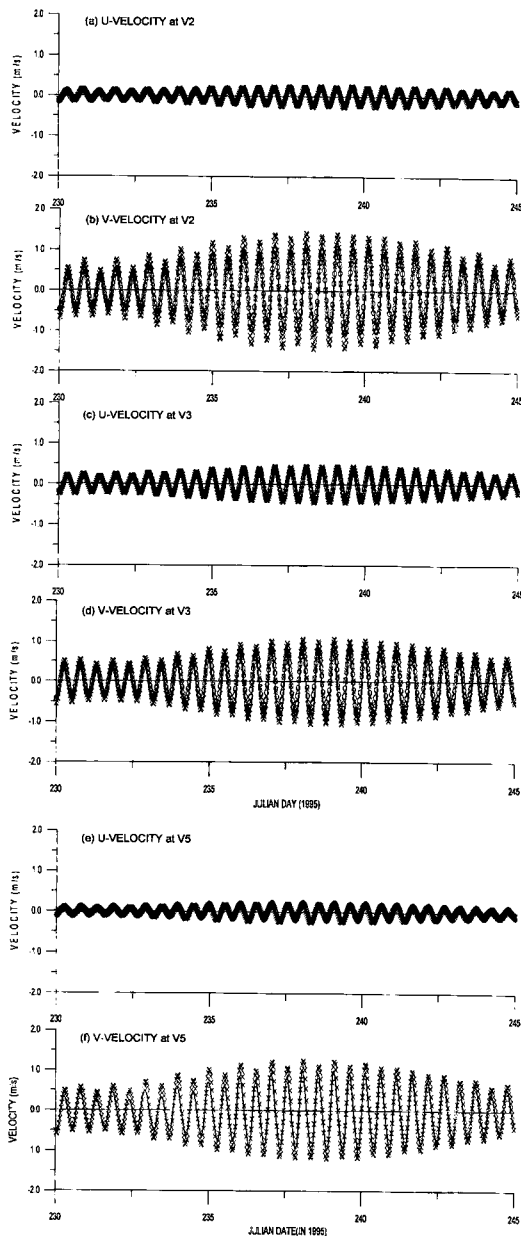


**Fig. 7.** Verification results for current velocities: (a) u and (b) v at V2, (c) u and (d) v at V3 and (e) u and (f) v at V5. Solid lines are model results. Mean depth is 20 m at V2 and V3, and 15 m at V5. At V2 and V3, × and ○ marks are field data from surface (4 m depth) and bottom (16 m depth), respectively. At V5, × marks are field data from mid-depth (7.5 m depth).

that Fig. 7 compares the model-computed vertical average velocities with the observed ones at surface and bottom. The other is that the field data in Fig. 7

are purely harmonic, while the model results do contain both tidal and nonlinearity-induced residual components, although the latter may be quite smaller than the former in the study area. Fig. 7 shows in general a good model-field agreement for both current amplitudes and phases, although the model underestimates the tidal current amplitude at station V3 (Fig. 7f). The verification results in Figures 6 and 7 demonstrate that the model gives a satisfactory reproduction of tidal dynamics in the Chunsu Bay system, especially for phases of tides and tidal currents.

### 5. CONCLUSION

The currently available data for tides and currents in most Korean coastal waters do allow us to perform model calibration and verification to some degree, and this paper is an example attempt for model calibration and verification with preexisting field data. This paper presents the procedure and the results of model calibration and verification conducted for the Chunsu Bay system. A horizontal two-dimensional version of POM was modified in representing the bottom friction and the open boundary conditions, and to incorporate wetting-and-drying scheme for intertidal flats. The model was applied to the Chunsu Bay system with only the effects of tides, the dominant forcing in the study area, being considered. The model was calibrated for the Manning's friction coefficient using the average tidal characteristics at three locations from Tide Tables. The calibrated model was verified using the time-series measurements of surface elevation and current velocity in the summer of 1995. Both calibration and verification results demonstrate that the model is capable of reproducing the tidal dynamics in the Chunsu Bay system, and provide measures of the degree of reliability of the model application.

### ACKNOWLEDGMENTS

This study was supported partly by the academic research fund of Ministry of Education, Republic

of Korea (BSRI-96-5424), and partly by the G-7 Environmental Research Program, Ministry of Environment and Ministry of Science and Technology, Republic of Korea (Phase II). Computations in the present work were carried out using the CRAY C90 of the SERI Supercomputer Center.

## REFERENCES

- Asselin, R., 1972. Frequency filter for time integrations, *Mon. Wea. Rev.*, **100**(6), pp. 487-490.
- Blumberg, A.F. and Mellor, G.L., 1987. A description of a three-dimensional coastal ocean circulation model, In: *Three-dimensional Coastal Ocean Models* edited by N.S. Heaps, AGU, Washington, D.C., pp. 1-16.
- Cheng, R.T., Casulli, V. and Gartner, J.W., 1993. Tidal, residual, intertidal mudflat (TRIM) model and its applications to San Francisco Bay, California, *Est. Coast. Shelf Sci.*, **36**, pp. 235-280.
- Daily, J.W. and Harleman, D.R.F., 1966. *Fluid dynamics*, Addison-Wesley, Massachusetts.
- Dronkers, J.J., 1964. *Tidal computations in rivers and coastal waters*, North-Holland, Amsterdam.
- Flather, R.A. and Heaps, N.S., 1975. Tidal computations for Morecambe Bay, *Geophys. J. R. Astr. Soc.*, **42**, pp. 489-517.
- Galperin, B. and Mellor, G.L., 1990. A time-dependent, three-dimensional model of the Delaware Bay and River system, Part 1: description of the model and tidal analysis, *Est. Coast. Shelf Sci.*, **31**, pp. 231-253.
- Jung, Y.-C. and Yoa, S.-J., 1992. Numerical modelling on hydrodynamics and diffusion in Suyeong Bay, *Bull. Korean Fish. Soc.*, **25**(2): 133-143 (in Korean).
- Kim, C.-K., 1994. Three-dimensional numerical model experiments of tidal and wind-driven currents in Chinhae Bay, *J. Korean Soc. Oceanogr.*, **29**(2): 95-106.
- Kim, C.-K., Chang S.-D. and Lee, J.-S., 1994. Two-dimensional hydraulic and numerical modeling of tidal currents in Chinhae Bay, *J. Korean Soc. Oceanogr.*, **29**(2): 83-94 (in Korean).
- Korea Electric Power Corporation (KEPCO), 1996. A report on field surveys and numerical model experiments for construction of Boryung Thermal Power Plant, KEPCO Report (in Korean).
- Korea Ocean Research and Development Institute (KORDI), 1996. Harmonic constants of tide around the Korea Peninsula, Republic of Korea (in Korean).
- KORDI, 1997. Development of coastal water quality assessment and prediction technology, Annual Report for Marine Environmental Monitoring and Assessment Technology, Ministry of Environment, Republic of Korea (in Korean).
- Kuo, A.Y. and Park, K., 1995. A framework for coupling shoals and shallow embayments with main channels in numerical modeling of coastal plain estuaries, *Estuaries*, **18**(2), pp. 341-350.
- Lee, B.-G., 1994. A study of physical oceanographic characteristics of Deukryang Bay using numerical and analytical models in summer, Ph.D. Dissertation, National Fisheries University of Pusan, Pusan.
- Leendertse, J.J. and Gritton, E.C., 1971. A water-quality simulation model for well mixed estuaries and coastal seas: Vol. 2, Computation procedure, *Rep. No. R-708-NYC*, The Rand Corporation, New York.
- Mellor, G.L., 1996. *Users guide for a three-dimensional, primitive-equation numerical ocean model*, Program in Atmospheric and Oceanic Sciences, Princeton University, New Jersey.
- Oey, L.-Y., Mellor G.L. and Hires, R.I., 1985. A three-dimensional simulation of the Hudson-Raritan Estuary, Part I: Description of the model and model simulations, *J. Phys. Oceanogr.*, **15**(12), pp. 1676-1692.
- Office of Hydrographic Affairs, 1992. Tidal current charts (Kyongnyolbi Yolto Approaches), Publication No. 1433, Republic of Korea.
- Park, K., Kuo A.Y., and Neilson, B.J., 1991. Calibration and verification of a water quality model for tidal estuary, In: *Proc. International Conf. on Computer Applications in Water Resources* edited by S.L. Yu and K.K. Shih, Tamshui, Taiwan, pp. 443-450.
- Park, K. and Kuo, A.Y., 1994. Numerical modelling of advective and diffusive transport in tidal Rappahannock Estuary, Virginia, In: *Estuarine and Coastal Modeling III* edited by M.L. Spaulding, K.W. Bedford, A.F. Blumberg, R.T. Cheng and J.C. Swanson, ASCE, New York, pp. 461-474.
- Park, K., 1996. Concept of surface water quality modeling in tidal rivers and estuaries, *Environ. Eng. Res.*, **1**(1), pp. 1-13.

- Park, K., Kuo A.Y. and Neilson, B.J., 1996. A numerical model study of hypoxia in the tidal Rappahannock River of Chesapeake Bay, *Est. Coast. Shelf Sci.*, **42**(5), pp. 563-581.
- Pugh, D.T., 1987. *Tides, surges and mean sea-level*, John Wiley & Sons, New York.
- Smagorinsky, J., 1963. General circulation experiments with the primitive equation, I. the basic experiment, *Mon. Wea. Rev.*, **91**, pp. 99-164.
- Yoo, I.-H., 1992. Numerical modelling of current and diffusion in Cheonsu Bay and its adjacent waters, Master Thesis, Chungnam National University, Taejon (in Korean).